WATER RESEARCH 46 (2012) 5696–5706

Available online at www.sciencedirect.com

SciVerse ScienceDirect

journal homepage: www.elsevier.com/locate/watres

Competition between kaolinite flocculation and stabilization in divalent cation solutions dosed with anionic polyacrylamides

Byung Joon Lee [a,c], *Mark A. Schlautman* [b,*], *Erik Toorman* [a], *Michael Fettweis* [c]

[a] *Hydraulics Laboratory, Department of Civil Engineering, Katholieke University of Leuven, Kasteelpark Arenberg 40, B-3001 Heverlee, Belgium*

[b] *Department of Environmental Engineering and Earth Sciences, Clemson University, 342 Computer Court, Anderson, SC 29625-6510, USA*

[c] *Management Unit of the North Sea Mathematical Models (MUMM), Royal Belgian Institute of Natural Sciences, Gulledelle 100, 1200 Brussels, Belgium*

ARTICLE INFO

Article history:
Received 17 May 2012
Received in revised form
24 July 2012
Accepted 28 July 2012
Available online 11 August 2012

Keywords:
Flocculation
Stabilization
Polyelectrolyte
Colloid
Divalent cation
Cationic bridge

ABSTRACT

Divalent cations have been reported to develop bridges between anionic polyelectrolytes and negatively-charged colloidal particles, thereby enhancing particle flocculation. However, results from this study of kaolinite suspensions dosed with various anionic polyacrylamides (PAMs) reveal that Ca^{2+} and Mg^{2+} can lead to colloid stabilization under some conditions. To explain the opposite but coexisting processes of flocculation and stabilization with divalent cations, a conceptual flocculation model with (1) particle-binding divalent cationic bridges between PAM molecules and kaolinite particles and (2) polymer-binding divalent cationic bridges between PAM molecules is proposed. The particle-binding bridges enhanced flocculation and aggregated kaolinite particles in large, easily-settleable flocs whereas the polymer-binding bridges increased steric stabilization by developing polymer layers covering the kaolinite surface. Both the particle-binding and polymer-binding divalent cationic bridges coexist in anionic PAM- and kaolinite-containing suspensions and thus induce the counteracting processes of particle flocculation and stabilization. Therefore, anionic polyelectrolytes in divalent cation-enriched aqueous solutions can sometimes lead to the stabilization of colloidal particles due to the polymer-binding divalent cationic bridges.

1. Introduction

Polyelectrolytes are linear polymeric molecules with repeating units of ionized functional groups on their backbone, and they can be negatively or positively charged depending on the specific functional groups present (Sperling, 2006). Most natural polyelectrolytes are produced by a myriad of biological processes and are weakly acidic and anionic under ambient aqueous solution conditions because of the hydrolyzable functional groups on their backbone. Extracellular polymeric substances produced by microorganisms are a typical example of natural anionic polyelectrolytes in the water environment (Droppo et al., 2005). Many synthetic polyelectrolytes also have been developed as biomimetic anionic polyelectrolytes, including anionic polyacrylamides (commercially known as PAM) (Myagachenkov and Kurenkov, 1991; Seybold, 1994; Orts et al., 2007).

---

[*] *Corresponding author*. Tel.: +1 864 656 4059; fax: +1 864 656 0672.
E-mail address: mschlau@clemson.edu (M.A. Schlautman).

0043-1354/$ – see front matter © 2012 Elsevier Ltd. All rights reserved.
http://dx.doi.org/10.1016/j.watres.2012.07.056

Natural and synthetic anionic polyelectrolytes are capable of binding colloidal particles together in large flocs, thereby enhancing particle flocculation. For example, extracellular polymeric substances enhance soil/sediment flocculation in rivers, lakes and estuaries (De Brouwer et al., 2002; Chen et al., 2005; Droppo et al., 2005; Lee et al., 2011). Anionic PAMs, which can be thought of as synthetic analogs of extracellular polymeric substances, have been used widely as flocculating agents to control soil erosion and sediment runoff from source sites and to remove suspended solids in water and wastewater treatment processes (Roa-Espinosa et al., 2000; Lentz et al., 2002; Lu et al., 2003; McLaughlin and Bartholomew, 2007; Sojka et al., 2007).

Addition of anionic polyelectrolytes to aqueous colloidal suspensions leads to the consecutive physicochemical processes of polyelectrolyte adsorption on colloidal particles and subsequent polyelectrolyte-mediated flocculation (Gregory, 1988; Pelssers et al., 1989; Lu and Pelton, 2001). Although both anionic polyelectrolytes and many colloidal particles are negatively charged, adsorption and polyelectrolyte-mediated flocculation occur because hydrogen bonding, van der Waals attractions, and/or sporadic cationic sites on the particle surfaces are able to overcome any initial electrostatic repulsion (Barvenik, 1994; Seybold, 1994; Stumm and Morgan, 1996; Mpofu et al., 2003; Sylvia et al., 2003).

Divalent cations such as Ca^{2+} or Mg^{2+} can be highly effective at reducing the electrostatic repulsion between anionic polyelectrolytes and negatively-charged colloidal particles, thereby enhancing polyelectrolyte adsorption and polyelectrolyte-mediated flocculation (Mpofu et al., 2003; Orts et al., 2007; Plach et al., 2011). Divalent cations not only reduce the electrostatic repulsion between negatively-charged colloidal particles themselves, but also provide anchoring and bridging sites for anionic polyelectrolyte molecules. They consequently enhance polyelectrolyte adsorption and polyelectrolyte-mediated flocculation by building divalent cationic bridges between polyelectrolyte molecules and colloidal particles (e.g., represented as $\text{Colloid}^{-}\cdots{}^{+}\text{M}^{+}\cdots{}^{-}\text{Polymer}^{-}\cdots{}^{+}\text{M}^{+}\cdots{}^{-}\text{Colloid}$) and forming large flocs with the colloidal particles. For example, Lu et al. (2002) reported that divalent cations can increase adsorption of anionic polyelectrolytes by soil/sediment particles up to nearly 30 times higher than monovalent cations. Polyelectrolyte-mediated flocculation of soil/sediment particles also has been reported to increase due to the divalent cationic bridges for binding colloidal particles (Entry et al., 2002; McLaughlin and Bartholomew, 2007; Orts et al., 2007; Mietta, 2010).

Although divalent cationic bridges are commonly reported to enhance anionic polyelectrolyte-mediated flocculation, there may be conditions under which divalent cations can reduce the efficacy of flocculation and instead enhance colloid stability. For example, divalent cationic bridges between anionic polyelectrolyte molecules have been identified which can build larger structures in solution (Sabbagh and Delsanti, 2000; Abraham et al., 2001). Similar bridges may also occur between adsorbed anionic polyelectrolyte molecules on colloidal particle surfaces, which would reduce flocculation and enhance particle stabilization due to the polymeric "coating" on the colloid surface.

The main objective of this research was to investigate the effects of Ca^{2+} and Mg^{2+} on the adsorption of PAM by kaolinite and on the subsequent flocculation/stabilization of kaolinite. A series of anionic PAMs with different charge densities (10–50%) and molecular weights (3.2–4.7 × 10^6 g/mol) were used as model compounds for natural and synthetic anionic polyelectrolytes. A new conceptual model of divalent cation-polyelectrolyte bridges on the kaolinite surface as well as between kaolinite particles was developed based on the experimental results and analysis and used to explain the counteracting processes of particle stabilization and flocculation.

2. Materials and methods

2.1. Anionic PAMs

Five anionic PAM samples with different molecular weights (MWs) and charge densities (CDs) were obtained from Kemira Water Solutions Inc. (Lakeland, FL) (Table 1). To remove salts

Table 1 – Vendor-provided characteristics and measured values for the molecular weights and charge densities of anionic PAMs utilized in this study.

PAM	Vendor provided value		Measured value			
	Molecular weight	Charge density (%)	[a]MW_V (10^6 g/mol)	[b]MW_W (10^6 g/mol)	[c]CD (%)	[d]COO-(mmol/g-PAM)
A100H	High	10	2.73 ± 0.069	4.71 ± 0.12	11.4 ± 0.06	1.61
A120	Medium	20	1.86 ± 0.058	3.20 ± 0.10	25.5 ± 0.26	3.59
A120H	High	20	3.27 ± 0.098	5.63 ± 0.17	25.2 ± 0.07	3.55
A150L	Low	50	1.97 ± 0.051	3.40 ± 0.09	51.1 ± 0.10	7.20
A150	Medium	50	2.49 ± 0.072	4.30 ± 0.12	45.8 ± 0.47	6.45

a Viscosity-averaged molecular weights (MW_V) were measured by the intrinsic viscosity measurement technique (Wu et al., 1991; Lee et al., 2010).

b Weight-averaged molecular weights (MW_W) were estimated with viscosity-averaged molecular weights (MW_V) with applying the conversion factor ($MW_W = 1.724 \times MW_V$) (Lee et al., 2010).

c Charge densities were measured by the potentiometic acid-base titration (Lee et al., 2010).

d Carboxylic groups per g PAM (=CD(%)/7.1).

and other impurities (mostly NaCl), the PAMs were purified by repeated dissolution, acidification and precipitation in water-methanol mixtures (Francois et al., 1979). First, 5 g of a commercial PAM powder was added to 1 L of distilled deionized water (DDW) and gently mixed on a Thermolyne® Bigger Bill orbital shaker (Thermo Fisher Scientific Inc., PA) for one to two days following a previously reported procedure (Francois et al., 1979). After complete dissolution, the PAM solution was acidified to pH 3 with hydrochloric acid to protonate the PAM functional groups and dissociate cations. Methanol was then added and the PAM precipitated at 4 °C. The sequence of PAM dissolution, acidification and precipitation was repeated four or five times. Finally, the precipitated PAM was freeze dried (VirTis®, SP Industries Inc.) and stored in powder form for later use. The PAM molecular weights and charge densities were determined as reported previously (Wu et al., 1991; Lee et al., 2010). Prior to adsorption and flocculation tests, aqueous stock solutions of PAM (2 g/L) were prepared by dissolving the freeze-dried powders in DDW and storing them in the dark when not being used.

2.2. *Adsorption and flocculation tests*

A standard JarTester (PB-700™, Phipps & Bird Inc.) was used for the adsorption and flocculation tests in aqueous kaolinite suspensions dosed with PAM and divalent cations. The jar tests were designed to simulate adsorption and flocculation in waters containing polymeric substances and suspended sediments, such as a flocculant-aided sediment retention pond treating turbid water runoff or a natural water containing high concentrations of suspended cohesive sediment. Kaolinite (Sigma–Aldrich, MO) was used as the model colloid/clay particle because of its small size and overall negative surface charge. Kaolinite suspensions and PAM stock solutions were prepared separately before the adsorption and flocculation tests. Each kaolinite suspension was prepared at 20 g/L in aqueous solutions with different background salts, adjusted to a pH of 7, and then mixed for two days to equilibrate the suspension. The different background salt concentrations used were 1 mM $CaCl_2$, 1 mM $MgCl_2$, and 3 mM NaCl, all of which thus had an ionic strength of 3 mM. Immediately before the adsorption and flocculation tests, PAM solutions at six different concentrations were prepared by diluting stock aliquots with pH 7 aqueous solutions containing the appropriate salt type and concentration to match the corresponding kaolinite suspension. Then, 250 mL of kaolinite suspension and the same volume of diluted PAM solutions were rapidly mixed together in the six jars of the tester. After 6 h mixing at 150 rpm, enough for adsorption and flocculation to reach a steady state (Morris et al., 2002), a representative sample of flocs was carefully taken from each jar and fixed in an agar plate to measure floc size as described below. After an additional period (1 h) of settling without mixing, a supernatant aliquot was taken from each jar to determine the amount of PAM adsorbed to kaolinite, the residual suspended solids concentration, the Ca^{2+} or Mg^{2+} solid-phase concentration, and the zeta potential of residual colloids. Each jar test condition was replicated three times to assess uncertainty, quality assurance and experimental control. Therefore, all error bars shown in the figures of this paper represent the standard errors of three independent tests conducted under the same experimental conditions.

2.3. *Measurements of experimental indices*

To determine the concentration of PAM adsorbed on kaolinite, the solid-phase was separated from solution by centrifuging at 10,000 g for 20 min (Sorvall Evolution RC, Thermo Fisher Scientific Inc.). Solution-phase PAM concentrations were then measured with a TOC-V_{CSH} TOC/TN analyzer (Shimadzu Corp., Japan) and the adsorbed PAM concentrations (mg-PAM/g-kaolinite) calculated by mass balance. Residual suspended solids concentrations were determined following Standard Methods 2540D, Total Suspended Solids (APHA, 1998). Each sample aliquot taken after 1 h settling was filtered through a pre-weighed (MX5 microbalance, Mettler-Toledo Inc., OH, USA) 0.1 μm Supor® membrane filter (Pall Corp., US). The filter with its collected solids was then dried at 105 °C, reweighed and the mass of collected solids determined by difference.

The floc fixation method utilized agar plates and photographic image processing to measure the size and morphology of flocs. At the end of 6 h mixing, suspended flocs were removed from the jar tester with a spatula and immediately fixed on a liquefied agar plate. Because the flocs had matured and ripened to a steady state condition under relatively high mixing conditions, they were not altered by the gentle sampling procedure. The agar plate was then cooled to room temperature to solidify the gel and prevent further changes to the floc structure. This floc-embedding method in solidified agar has previously been shown to preserve the size and morphology of both biological and mineral flocs (Zahid and Ganczarczyk, 1990; Ganczarczyk et al., 1992; Gorczyca and Ganczarczyk, 1996). Microscopic images of the fixed flocs were recorded with a Sanyo VPC-HD2 Digital Media Camera (10 × optical zoom, 3072 × 2404 resolution, Sanyo Electric Co., Japan) equipped with a Tiffen close-up lens (The Tiffen Company, NY). The raw images were processed with public domain image processing software (Image J, National Institutes of Health, MD). Volume-averaged floc diameters were calculated with a built-in function in the software after first performing image processing (e.g., adjusting image contrast or brightness, deleting unclear floc images). At least 20 flocs (but at times up to 300 flocs, depending on the experimental conditions) were imaged on each agar plate and analyzed to estimate volume-averaged floc diameters. The steps of sampling, fixing and imaging of flocs were replicated three times for each jar test. Due to the resolution limit of the camera, the minimum measurable floc size was set at 50 μm. In other words, flocs smaller than 50 μm were deleted prior to calculating the volume-averaged floc diameter. Consequently, the volume-averaged floc diameters reported do not fully reflect the range of particle sizes that were present but instead are actually somewhat higher than the "true" volume-averaged diameters would have been. In this paper, we use the volume-averaged floc diameters primarily as a relative indicator of the flocculation capability for each test condition. On the other hand, residual suspended solid concentration was used as an indication of the mass fraction of particles/flocs below 50 μm diameter.

The apparent zeta potential of supernatant aliquots taken after 1 h of settling was measured with a Brookhaven ZetaPlus analyzer (Brookhaven Instruments Corp., NY, USA) and used to characterize the electrostatic conditions of kaolinite suspensions when dosed with the different PAMs in the different background salt solutions. Aliquots from each jar test were diluted with the appropriate background solution to minimize particle–particle interactions and overlapping during the actual zeta potential measurements. Zeta potentials for each aliquot were measured ten times and averaged to obtain more reliable values. Note that the zeta potentials we measured do not actually reflect the electrostatic properties of flocs that had formed and already settled from the suspensions during the jar tests. They are expected to be similar, however.

Solid-phase Ca^{2+} and Mg^{2+} concentrations were determined to investigate the effects of the divalent cations on PAM adsorption and PAM-mediated flocculation. The procedure utilized Standard Methods 2340C, EDTA titrimetric method (APHA, 1998). A small volume (1–2 mL) of the appropriate background solution and 1-2 drops of Calmagite indicator (0.1 w/v aqueous, VWR, USA) were added to a 50 mL centrifuged and filtered sample. The pH was raised to ~10 and the sample then titrated with 0.01 M standard EDTA solution (VWR, USA) to the end-point. The solution-phase Ca^{2+} or Mg^{2+} concentration was calculated based on the volume of titrant added

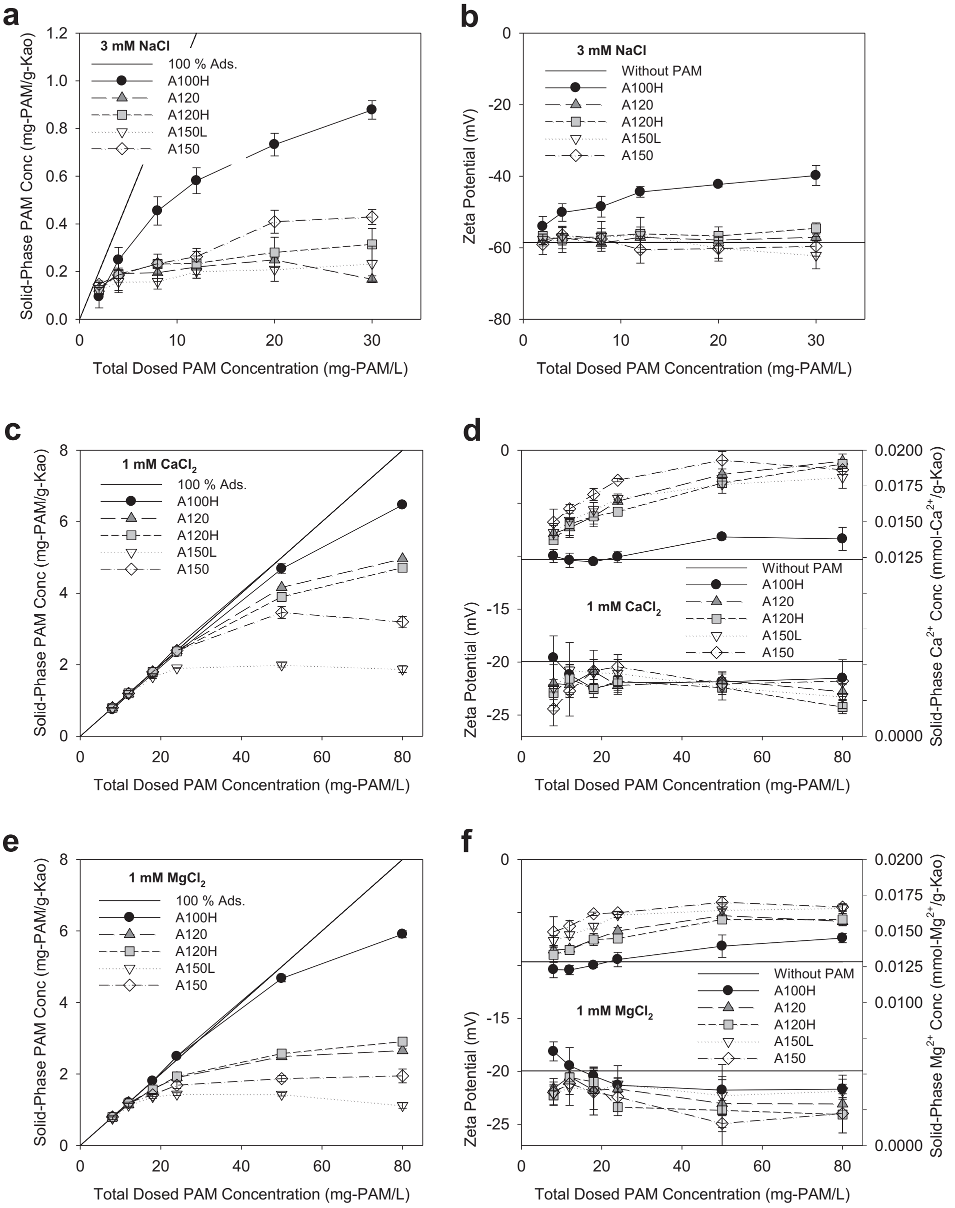

Fig. 1 – PAM adsorption (mg-PAM/g-Kaolinite) (a) and kaolinite zeta potentials (mV) (b) versus total PAM dosage (mg-PAM/L) in 3 mM NaCl solutions. PAM adsorption (c) and kaolinite zeta potentials (top) and solid-phase Ca^{2+} concentrations (bottom) (d) versus total PAM dosage in 1 mM $CaCl_2$ solutions. PAM adsorption (e) and kaolinite zeta potentials (top) and solid-phase Mg^{2+} concentrations (bottom) (f) versus total PAM dosage in 1 mM $MgCl_2$ solutions.

and the solid-phase concentration (mmol/g-Kaolinite) calculated by mass balance.

3. Results and discussion

3.1. *PAM and divalent cation adsorption by kaolinite and resulting zeta potentials*

The presence of 1 mM Ca^{2+} or Mg^{2+} greatly enhanced the adsorption of PAM by kaolinite relative to the 3 mM Na^{+} background solution (Fig. 1a, c and e). For all three background solutions, the solid-phase PAM concentration increased sharply initially but then reached/approached a plateau (i.e., maximum PAM adsorption capacity) with increasing PAM dose, consistent with a high-affinity adsorption behavior commonly reported for polymeric substances on surfaces (Fleer et al., 1993). For each of the background salt solutions, the adsorption behaviors of A120, A120 H, A150 L and A150 were similar. In contrast, the A100 H PAM tended to exhibit higher adsorption capacities and did not reach a clear plateau for the similar PAM dose used.

In the NaCl background solution, the A100 H again differed from the other PAM samples. For example, as the dose of A100 H increased the particle zeta potential continuously became less negative in the NaCl solution (Fig. 1b). For all the other PAM samples, however, the measured zeta potentials in the NaCl solution remained essentially constant and equal ($\zeta = -57.8 \pm 1.7$ mV (mean ± standard error), $n = 6 \times 4 = 24$ for combining all PAM types and doses tested) irrespective of the PAM dose and type. In the divalent cation solutions (Fig. 1d and f), all measured zeta potentials were essentially constant and equal for all PAM doses and types, including A100 H ($\zeta = -22.0 \pm 1.0$ and -21.9 ± 1.4 mV, $n = 6 \times 5 = 30$, for $CaCl_2$ and $MgCl_2$ solutions, respectively). These results will be discussed in more depth in Section 3.2.

In the absence of PAM, Ca^{2+} and Mg^{2+} adsorbed to the bare kaolinite surface with surface concentrations of 0.0124 ± 0.0004 and 0.0130 ± 0.0005 mmol/g-kaolinite, respectively. These two values are represented by the horizontal lines in Fig. 1d and f. With increasing PAM dose, the solid-phase Ca^{2+} and Mg^{2+} concentrations also increased before leveling out in a manner parallel to PAM adsorption.

Maximum PAM adsorption capacities/concentrations and the corresponding average zeta potentials in the three background salt solutions are plotted for comparison in Fig. 2. A general trend of decreasing maximum adsorption of PAM with increasing PAM anionic charge density (Table 1) can be observed, in the order of A100 H > A120 ≈ A120 H > A150 ≈ A150 L. However, the different maximum PAM adsorption capacities did not affect the average zeta potential measured in the different salt solutions (Fig. 2; also seen previously in Fig. 1b, d and f). In contrast, the valence of the salt cation present did affect measured zeta potentials, with the values in the presence of Ca^{2+} or Mg^{2+} being one third the magnitude of the (negative) zeta potential measured with Na^{+}. The two divalent cations not only decreased the negative zeta potential but also greatly increased the maximum PAM adsorption capacity, presumably by reducing the electrostatic repulsion between the anionic PAM molecules and the negatively-charged kaolinite particles (Stumm and Morgan, 1996). The following sections further elucidate the effects of PAM types and cation valence on kaolinite flocculation versus stabilization. In the figures that follow, the various experimental indices that we measured have been plotted as a function of both *solution* and *adsorbed* PAM concentration so that a fuller understanding of the processes involved can be revealed.

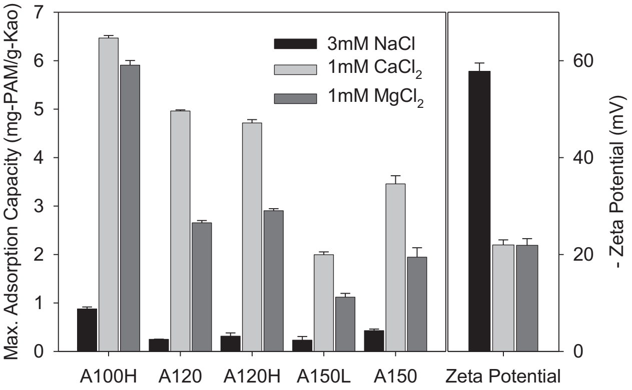

Fig. 2 – Maximum PAM adsorption capacities (mg-PAM/g-Kaolinite) and average kaolinite zeta potentials (mV) for the different PAM and cation combinations tested.

3.2. *Kaolinite flocculation vs. stabilization by PAMs in NaCl solution*

With increasing solution- (and therefore solid-phase) PAM concentration, kaolinite floc size decreased (Fig. 3a) and the residual suspended solid concentration increased (Fig. 3b) in solutions of 3 mM NaCl for all PAMs tested with the exception of A100 H. These results indicate that particle stabilization dominated over flocculation and minimized floc formation under these conditions. Electrostatic repulsion or steric stabilization is often invoked as the predominant process stabilizing particles with adsorbed polyelectrolytes (Bache and Gregory, 2007). However, considering that the zeta potential remained relatively constant for the kaolinite particles independent of PAM concentrations (Fig. 3c), electrostatic repulsion does not appear to explain our results. Instead, steric stabilization resulting from polyelectrolytes on the particle surface (Elimelech et al., 1995; Droppo et al., 2005; Bache and Gregory, 2007) better explains the enhanced stabilization observed for these PAM-coated kaolinite particles.

The A100 H PAM exhibited unique adsorption and flocculation/stabilization behaviors when compared to the other PAMs tested, which likely can be attributed to its large size and low charge density. For example, kaolinite floc size increased with increasing concentration of A100 H and reached a maximum at approximately 0.6 mg-PAM/g-kaolinite (Fig. 3a). In addition, the measured negative zeta potential decreased linearly with increasing solid-phase concentration of A100 H (Fig. 3c), suggesting that the additional PAM molecules being adsorbed were creating increasingly thick adsorbed layers on kaolinite. This led to enhanced screening of the electrostatic repulsion between particles and made

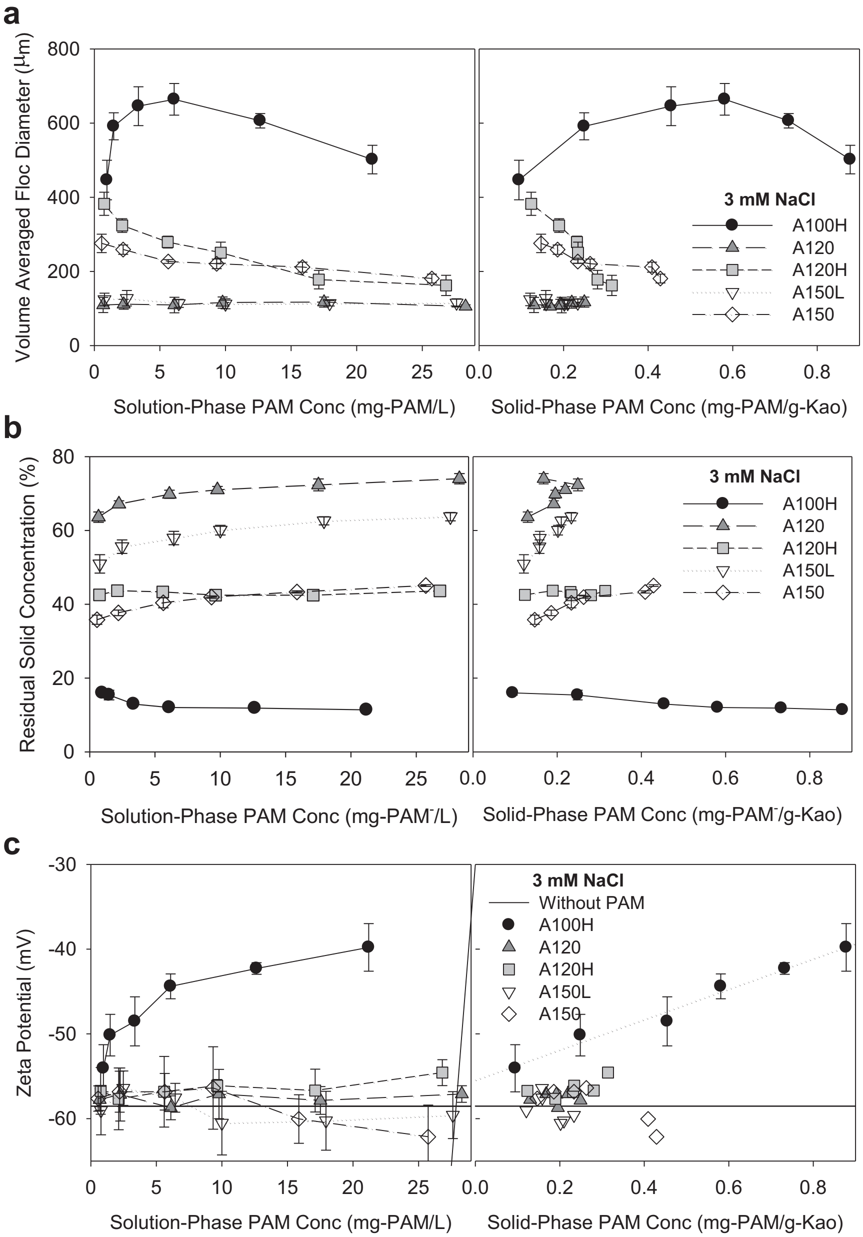

Fig. 3 – Volume-averaged floc diameter (μm) (a), non-settleable suspended solids concentration ($C_{residual}/C_{initial}$; %) (b), and kaolinite zeta potential (mV) (c) versus solution-phase PAM concentration (left panels) and adsorbed PAM concentration (right panels) in 3 mM NaCl.

flocculation dominant over stabilization with increasing concentration of A100 H. However, once the floc size reached a maximum, further increases in A100 H concentration resulted in smaller flocs due to particle stabilization becoming more important than particle flocculation.

3.3. *Kaolinite flocculation vs. stabilization by PAMs in divalent cation solutions*

Kaolinite floc sizes and residual solid concentrations in the presence of 1 mM divalent cations revealed a combination of general and unique behaviors, indicative of the counteracting processes of particle flocculation and stabilization (Fig. 4). In general, kaolinite floc size increased dramatically with very small increases in PAM solution-phase concentrations but then became constant or even decreased as solution-phase PAM concentrations increased further (Fig. 4, left panels). Examining kaolinite floc size as a function of solid-phase PAM concentration, however, provides more clarity to these results (Fig. 4, right panels) – now it becomes clearer that kaolinite floc size steadily increases with increasing amounts of adsorbed PAM molecules up to a unique maximum value before decreasing again. These results agree conceptually with the polymer-induced flocculation and stabilization

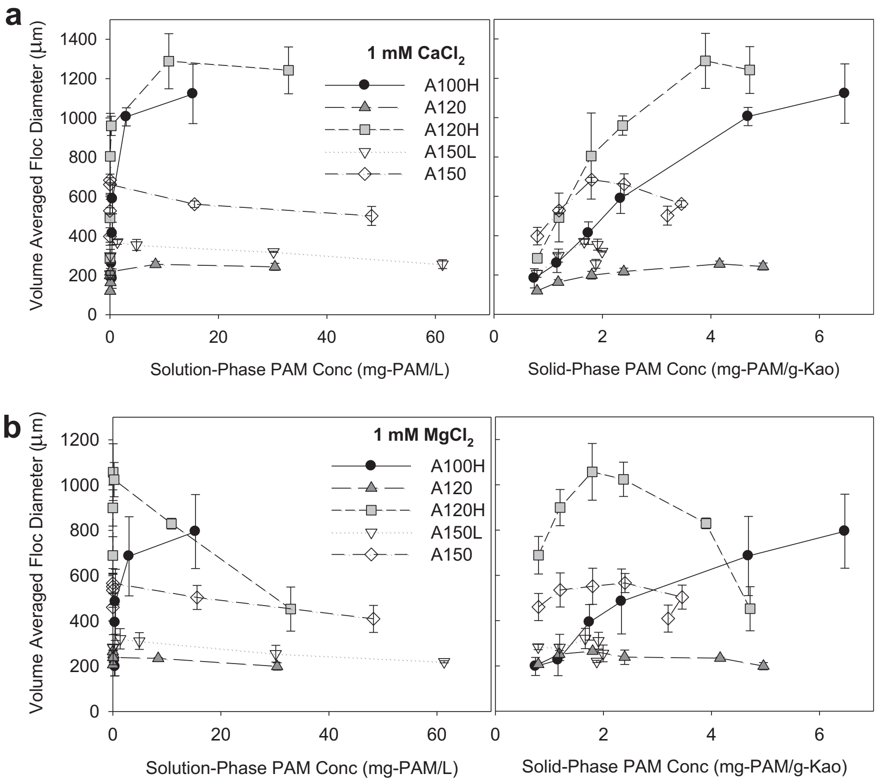

Fig. 4 – **Volume-averaged floc diameter (µm) versus solution-phase PAM concentration (left panels) and adsorbed PAM concentration (right panels) for kaolinite suspensions dosed with PAMs in 1 mM $CaCl_2$ solutions (a) or 1 mM $MgCl_2$ solutions (b).**

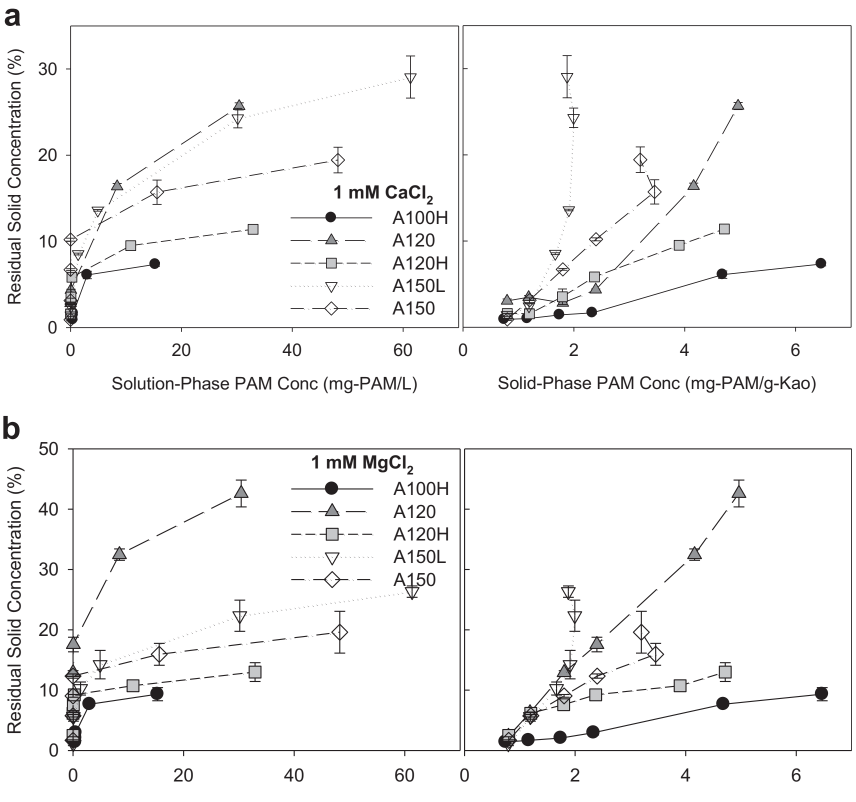

Fig. 5 – **Non-settleable suspended solids concentration ($C_{residual}/C_{initial}$; %) versus solution-phase PAM concentration (left panels) and adsorbed PAM concentration (right panels) for kaolinite suspensions dosed with PAMs in 1 mM $CaCl_2$ solutions (a) or 1 mM $MgCl_2$ solutions (b).**

mechanisms proposed by La Mer and Healy (Healy and La Mer, 1962, 1964; La Mer and Healy, 1963). In other words, when polyelectrolyte molecules attach to high-affinity adsorption sites they enhance particle flocculation by developing bridges between polymers and particles. Once all the high-affinity adsorption sites are occupied, however, further increases in PAM dose result in less and less favorable adsorption and higher concentrations of nonadsorbed PAM molecules in solution. This, in turn, reduces particle flocculation because the polymeric bridges become less favorable.

Concentrations of residual (i.e., non-settleable) kaolinite particles increased with increasing concentrations of PAM in solution in the presence of divalent cations (Fig. 5, left panels). When examined as a function of solid-phase PAM concentrations, one can see that the residual kaolinite concentrations increase with increasing concentrations of adsorbed PAM (Fig. 5, right panels). Therefore, colloid stabilization occurred at all PAM concentrations tested and steadily increased with increasing solid-phase PAM concentrations.

Divalent cations are widely reported to enhance particle flocculation by facilitating development of bridges between anionic polyelectrolytes and negatively-charged colloids (Droppo et al., 2005; Orts et al., 2007). However, results from this study reveal that divalent cations may enhance particle flocculation under some conditions but can also lead to particle stabilization in kaolinite suspensions when dosing with anionic PAM molecules. For example, floc sizes increased up to their maximum values in our 1 mM $CaCl_2$ or $MgCl_2$ solutions but then decreased as the adsorbed concentrations of PAM increased (Fig. 4, right panels), whereas the non-settleable solids concentrations continuously increased (Fig. 5, right panels). In other words, kaolinite flocculation and stabilization were equally effective at the lower solid-phase PAM concentrations but stabilization eventually dominated over flocculation at higher solid-phase PAM concentrations after passing the maximum floc size. These results defy conventional wisdom whereby scientists and engineers report only the advantageous role of divalent cations on polyelectrolyte-mediated flocculation. The following section discusses in more detail the heretofore unacknowledged role of divalent cations in bringing about particle stabilization rather than flocculation by examining measured zeta potentials of PAM-coated kaolinite particles and the corresponding solid-phase Ca^{2+} or Mg^{2+} concentrations.

3.4. *Two types of divalent cationic bridges*

Solid-phase Ca^{2+} and Mg^{2+} concentrations paralleled the high-affinity PAM adsorption trends when plotted against solution-phase PAM concentrations (Fig. 6, left panels). As expected, Ca^{2+} and Mg^{2+} adsorption were found to be highly correlated with PAM adsorption on kaolinite (Fig. 6, middle panels). Furthermore, with the exception of the A100 H PAM, adsorbed Ca^{2+} and Mg^{2+} concentrations could be normalized for the different PAMs tested by plotting them against the carboxyl group content of the adsorbed PAM species (Fig. 6,

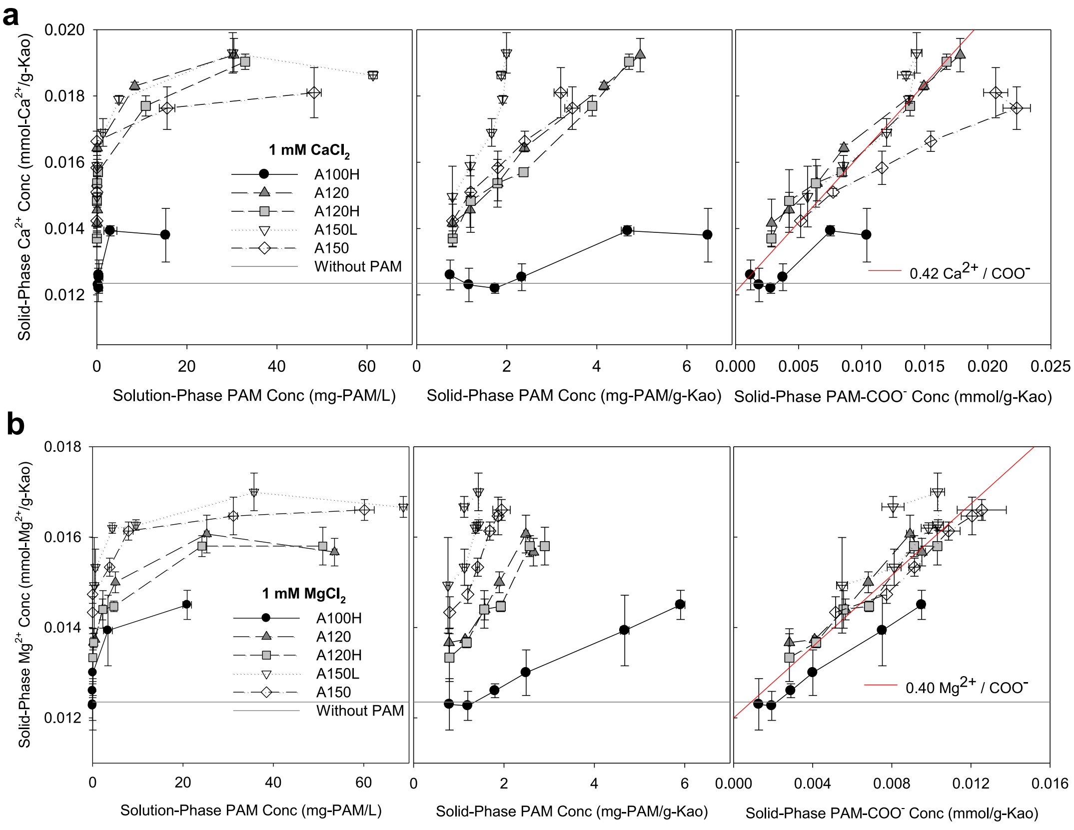

Fig. 6 – Solid-phase divalent cation concentrations (mmol/g-Kaolinite) versus solution-phase PAM concentration (left panels), adsorbed PAM concentration (middle panels) and solid-phase PAM carboxyl group concentration (right panels) for kaolinite suspensions dosed with PAMs in 1 mM $CaCl_2$ solutions (a) or 1 mM $MgCl_2$ solutions (b).

right panels). The adsorbed Ca^{2+} and Mg^{2+} concentrations increased proportionally with the solid-phase PAM carboxyl group concentrations, starting from the adsorbed cation concentrations in the absence of any PAM as represented by the solid horizontal lines in Fig. 6. Thus, it appears that the divalent cations adsorbed first on the bare kaolinite surface and then associated proportionally to the subsequent adsorption of PAM molecules. However, A150 PAM with Ca^{2+} gradually deviated from the generalized pattern shown with the other flocculants (i.e., 0.42 Ca^{2+}/COO^{-}) with increasing solid-phase PAM-COO^{-} concentration. We suspect that the adsorbed A150 PAM molecules might have become more compacted by adsorbed Ca^{2+} ions and therefore may have hindered subsequent access and adsorption of additional Ca^{2+} ions. Because Ca^{2+} has a higher electrostatic affinity (i.e., a smaller hydrated radius) than Mg^{2+}, a similar effect was not seen with Mg^{2+} and the A150 PAM.

The proportion of adsorbed divalent cations to PAM carboxyl group content in the adsorbed layer was 0.42 Ca^{2+}/COO^{-} and 0.40 Mg^{2+}/COO^{-}, respectively, which are both close to the theoretical charge balance of 0.5 Me^{2+}/COO^{-}. The co-adsorption of divalent cations and PAM molecules at a ratio that roughly balances their opposite charges helps explain why measured zeta potentials of PAM-coated kaolinite particles remained relatively constant despite the increasing adsorbed concentrations of PAM (Fig. 7). Furthermore, it reveals that the electrostatic properties of PAM-coated kaolinite did not affect particle flocculation and stabilization. Rather, it appears that formation of the co-adsorbed polyelectrolyte and divalent cation coating on kaolinite is a key factor controlling particle flocculation and/or stabilization.

As shown previously, the zeta potential of kaolinite in the absence of PAM was approximately −58 mV in 3 mM NaCl (Figs. 1b and 3c). In the 1 mM divalent cation salt solutions, however, the zeta potential of kaolinite in the absence of PAM became less negative: −20.0 ± 1.3 and −21.0 ± 0.7 mV (Mean ± Standard Error for three independent tests) for CaCl$_2$ and MgCl$_2$, respectively (i.e., dotted lines in Fig. 7). However, when different PAMs were dosed at different concentrations into the kaolinite suspensions that contained CaCl$_2$ and MgCl$_2$, we found that the two divalent cations had little to no effect on the particle zeta potentials. Although the measured zeta potentials of PAM-coated kaolinite were slightly more negative than the PAM-free kaolinite particles (Fig. 7), the difference was not significant at the 95% confidence level. The fact that the zeta potentials of PAM-coated kaolinite had no statistically significant correlation with PAM carboxyl concentrations in the adsorbed layer supports the idea that electrostatic properties are not controlling particle flocculation or stabilization in our experimental systems containing kaolinite, divalent cations, and various types and doses of PAM.

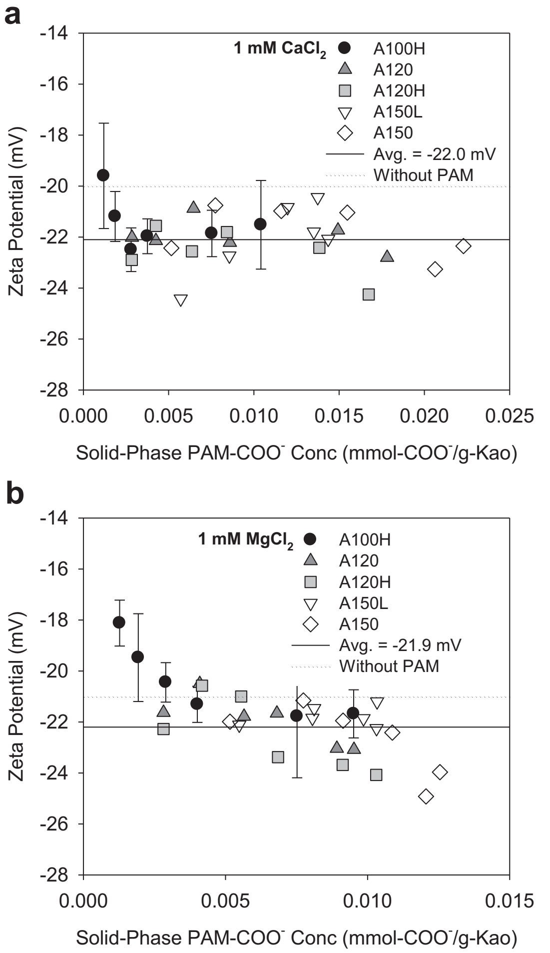

Fig. 7 – Kaolinite zeta potential (mV) versus solid-phase PAM carboxyl group concentration for kaolinite suspensions dosed with PAMs in 1 mM CaCl$_2$ solutions (a) or 1 mM MgCl$_2$ solutions (b). Error bars for PAMs, which have been omitted for clarity, ranged from 0.1 to 2.7 mV (also see Fig. 1).

A conceptual model can be proposed to describe the formation of an adsorbed polymeric layer consisting of anionic PAM molecules and divalent cations and the concurrent, counteracting processes of particle flocculation and stabilization in our experimental systems specified by the chemical and mineral components as well as the order of adding the components (Fig. 8). This conceptual model includes two different types of divalent cationic bridges: (1) a particle-binding bridge between PAM molecules and kaolinite particles (e.g., $\text{Kao}^{-} - {}^{+}\text{M}^{+} - {}^{-}\text{OOC} \sim \text{PAM} \sim \text{COO}^{-} - {}^{+}\text{M}^{+} - {}^{-}\text{Kao}$) and (2) a polymer-binding bridge between PAM molecules (e.g., $\text{PAM} \sim \text{COO} - {}^{+}\text{M}^{+} - {}^{-}\text{OOC} \sim \text{PAM}$). The particle-binding divalent cationic bridge would be formed by the serial processes of divalent cations, such as adsorption on bare kaolinite, reduction of electrostatic repulsion between kaolinite and anionic PAM carboxylic groups, and development of PAM-bridging sites on kaolinite. The particle-binding divalent cationic bridge thus enhances particle flocculation because it holds kaolinite particles together in large settleable flocs. Simultaneously, the polymer-binding divalent cationic bridge would be formed between adjacent carboxylic groups of PAM molecules adsorbed on kaolinite, and therefore would enhance particle stabilization by developing a saturated polymeric layer on kaolinite, blocking the particle-binding bridge and keeping kaolinite particles apart. Particle flocculation prevails for the lower solid-phase PAM concentrations, probably due to the larger number of particle-binding bridges that occupy the high affinity adsorption sites on kaolinite. However, stabilization

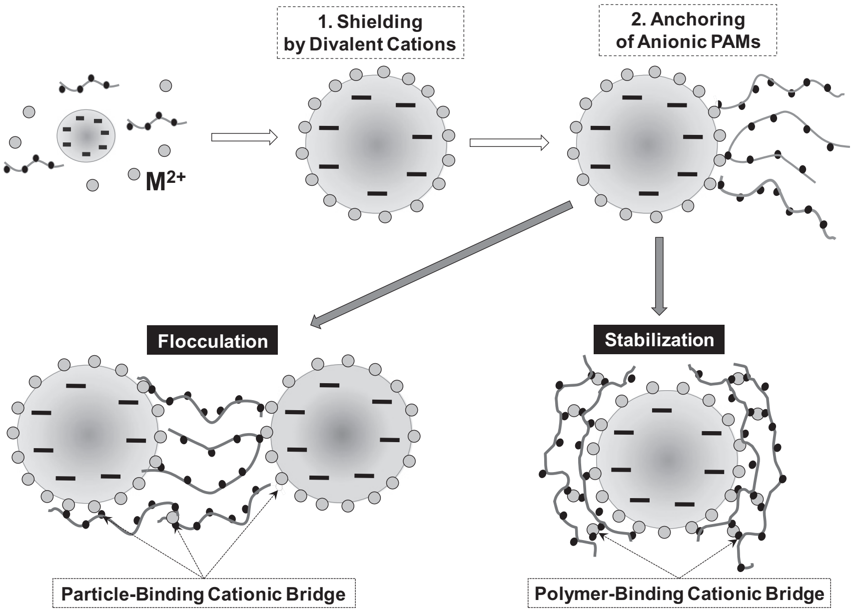

Fig. 8 – Schematic diagram illustrating conceptual model of PAM adsorption on kaolinite and PAM-mediated particle flocculation for two different types of divalent cationic bridges.

begins to dominate over flocculation at higher solid-phase PAM concentrations due to a larger number of polymer-binding bridges that block other high affinity adsorption sites. The particle-binding and the polymer-binding bridges surely coexist in kaolinite suspensions with anionic PAMs and divalent cations and thus lead to the competitive effects of particle flocculation and stabilization.

Aqueous solutions enriched in divalent cations have been reported to build bridges between polyacrylate molecules (e.g., PAA ~ $COO^- - {}^+M^+ - {}^-OOC$ ~ PAA, where PAA is polyacrylic acid) and develop saturated polymeric structures of polyacrylate molecules (Sabbagh and Delsanti, 2000; Abraham et al., 2001). Similarly, divalent cations can be concentrated on kaolinite surfaces by adsorption and thus be accessible to build similar bridges between anionic PAM molecules, thereby developing saturated polymeric layers on kaolinite. According to theories of steric stabilization (Healy and La Mer, 1964; Lu and Pelton, 2001; Bache and Gregory, 2007), saturated polymeric layers that block high-affinity adsorption sites on particles prevent the building of polymer-binding cationic bridges and therefore reduce particle flocculation. In addition, this new adsorbed layer could conceivably reduce the Hamaker constant and associated van der Waals attraction forces and result in enhanced particle stabilization (Stumm and Morgan, 1996; Bache and Gregory, 2007). In fact, the proposed model specifies flocculation and stabilization mechanisms in bridging flocculation, incorporating the roles of divalent cations for such bridging flocculation.

4. Conclusions and recommendations

The beneficial effects of divalent cationic bridges for polyelectrolyte-enhanced flocculation has been widely reported and utilized in many natural and engineered flocculation systems. This study, however, demonstrates that particle-binding and polymer-binding divalent cationic bridges have positive and negative effects, respectively, on the flocculation of colloidal particles. The conceptual model we have proposed for the two types of divalent cationic bridges is based on indirect evidence using conventional experimental indices such as adsorbed polyelectrolyte concentrations, adsorbed divalent cation concentrations, floc sizes, and non-settleable solids concentrations. More sophisticated microscopic and spectroscopic techniques will be needed in future studies to obtain direct evidence for these proposed bridges. Such direct measurements and new models of the processes involved will enable us in the future to better understand the roles of divalent cations in particle flocculation and stabilization in many natural and engineered systems containing colloidal particles and anionic polyelectrolytes.

Acknowledgments

We gratefully acknowledge the helpful comments provided by the reviewers. Primary funding for this study was provided by the USDA Natural Resources Conservation Service (NRCS-69-4639-1-0010) through the Changing Land Use and Environment (CLUE) Project at Clemson University. Additional support was provided by the USDA Cooperative State Research, Education, and Extension Service (USDA-CSREES) under project numbers SC-1700278, SC-1700395 and SC-1700427. Any opinions, findings, conclusions or recommendations expressed in this article are solely those of the authors and do not necessarily reflect the views of the USDA. Author Lee also acknowledges financial support from the Clemson University Department of Environmental Engineering and Earth Sciences (teaching assistantship and L.G. Rich Fellowship), the Clemson University Graduate School (R.C. Edwards Fellowship), and for his postdoctoral study from the Flemish

Science Foundation (FWO project no. G.0263.08) and the OMFLOC project (Royal Belgian Institute of Natural Sciences – MUMM). This is Technical Contribution No. 6065 of the Clemson University Experiment Station.

REFERENCES

Abraham, T., Kumpulainen, A., Xu, Z., Rutland, M., Claesson, P., Masliyah, J., 2001. Polyelectrolyte-mediated interaction between similarly charged surfaces: role of divalent counter ions in tuning surface forces. Langmuir 17, 8321–8327.

APHA, 1998. Standard Methods for the Examination of Water and Wastewater, twentieth ed. American Public Health Association, USA.

Bache, D.H., Gregory, R., 2007. Flocs in Water Treatment. IWA Publishing, Alliance House, 12 Caxton Street, London, UK.

Barvenik, F., 1994. Polyacrylamide characteristics related to soil applications. Soil Science 158, 235–243.

Chen, M., Wartel, S., Temmerman, S., 2005. Seasonal variation of floc characteristics on tidal flats, the Scheldt estuary. Hydrobiologia 540, 181–195.

De Brouwer, J., Ruddy, G., Jones, T., Stal, L., 2002. Sorption of EPS to sediment particles and the effect on the rheology of sediment slurries. Biogeochemistry 61, 57–71.

Droppo, I., Leppard, G., Liss, S., Milligan, T., 2005. Flocculation in Natural and Engineered Environmental Systems. CRC Press Inc., Boca Raton, Florida, USA.

Elimelech, M., Gregory, J., Jia, X., Williams, R., 1995. Particle Deposition and Aggregation: Measurement, Modeling, and Simulation. Butterworth-Heinemann, Oxford.

Entry, J., Sojka, R., Watwood, M., Ross, C., 2002. Polyacrylamide preparations for protection of water quality threatened by agricultural runoff contaminants. Environmental Pollution 120, 191–200.

Fleer, G., Cohen Stuart, M., Scheutjens, J., Cosgrove, T., Vincent, B., 1993. Polymers at Interfaces. Chapman & Hall, London, UK.

Francois, J., Sarazin, D., Schwartz, T., Weil, G., 1979. Polyacrylamide in water: molecular weight dependence of $<R^2>$ and $[\eta]$ and the problem of the excluded volume exponent. Polymer 20, 969–975.

Ganczarczyk, J., Zahid, W., Li, D., 1992. Physical stabilization and embedding of microbial aggregates for light microscopy studies. Water Research 26, 1695–1699.

Gorczyca, B., Ganczarczyk, J., 1996. Image analysis of alum coagulated mineral suspensions. Environmental Technology 17, 1361–1369.

Gregory, J., 1988. Polymer adsorption and flocculation in sheared suspensions. Colloid & Polymer Science 31, 231–253.

Healy, T., La Mer, V., 1962. The adsorption-flocculation reactions of a polymer with an aqueous colloidal dispersion. Journal of Physical Chemistry 66, 1835.

Healy, T., La Mer, V., 1964. The energetics of flocculation and redispersion by polymers. Journal of Colloid Science 19, 323–332.

La Mer, V., Healy, T., 1963. The role of filtration in investigating flocculation and redispersion of colloidal dispersions. Journal of Physical Chemistry 67, 2417.

Lee, B., Ko, S., Luzinov, I., Hayes, J., Schlautman, M., 2010. Evaluating simple, low-cost techniques to estimate molecular weights and charge densities of polydisperse commercial polyacrylamides for soil and sediment applications. Transactions of the ASACE 53, 1127–1136.

Lee, B., Toorman, E., Molz, F., Wang, J., 2011. A two-class population balance equation yielding bimodal flocculation of marine or estuarine sediments. Water Research 45, 2131–2145.

Lentz, R., Sojka, R., Mackey, B., 2002. Fate and efficacy of polyacrylamide applied in furrow irrigation: full-advance and continuous treatment. Journal of Environmental Quality 34, 661–678.

Lu, C., Pelton, R., 2001. PEO Flocculation of polystyrene-core poly (vinylphenol)-shell latex: an example of ideal bridging. Langmuir 17, 7770–7776.

Lu, J., Wu, L., Letey, J., 2002. Effects of soil and water properties on anionic polyacrylamide sorption. Soil Science society of America Journal 66, 578–584.

Lu, J., Wu, L., Gan, J., 2003. Determination of polyacrylamide in soil waters by size exclusion chromatography. Journal of Environmental Quality 32, 1922–1926.

McLaughlin, R., Bartholomew, N., 2007. Soil factors influencing suspended sediment flocculation by polyacrylamide. Soil Science Society of America Journal 71, 537–544.

Mietta, F., 2010. Evolution of the Floc Size distribution of Cohesive Sediments. PhD dissertation, Delft University of Technology, The Netherlands.

Morris, G., Fornasiero, D., Ralston, J., 2002. Polymer depressants at the talc-water interface: adsorption isotherm, microflotation and electrokinetic studies. International Journal of Mineral Processing 67, 211–227.

Mpofu, P., Addai-Mensah, J., Ralston, J., 2003. Influence of hydrolyzable metal ions on the interfacial chemistry, particle interactions, and dewatering behavior of kaolinite dispersion. Journal of Colloid and Interface Science 261, 349–359.

Myagachenkov, V., Kurenkov, V., 1991. Applications of acrylamide polymers and copolymers: a review. Polymer-Plastics Technology and Engineering 30, 109–135.

Orts, W., Roa-Espinosa, A., Sojka, R., Glenn, G., Iman, S., Erlacher, K., Pedersen, J., 2007. Use of synthetic polymers and biopolymers for soil stabilization in agricultural, construction, and military applications. Journal of Materials in Civil Engineering 19, 58–66.

Pelssers, E., Cohen Stuart, M., Fleer, G., 1989. Kinetic aspects of polymer bridging: equilibrium flocculation and nonequilibrium flocculation. Colloids and Surfaces 38, 15–25.

Plach, J., Elliotte, A., Droppo, I., Warren, L., 2011. Physical and ecological controls on freshwater floc trace metal dynamics. Environmental Science and Technology 45, 2157–2164.

Roa-Espinosa, A., Bubenzer, G., Miyashita, E., 2000. Sediment and runoff control on construction sites using four application methods of polyacrylamide mix. In: Proceedings of National Conference on Tools for Urban Water Resource Management and Protection February 7, Chicago, IL.

Sabbagh, I., Delsanti, M., 2000. Solubility of highly charged anionic polyelectrolytes in presence of multivalent cations: specific interaction effect. The European Physical Journal E 1, 75–86.

Seybold, C., 1994. Polyacylamide review: soil conditioning and environmental fate. Communications in Soil Science and Plant Analysis 25, 2171–2185.

Sojka, R., Bjorneberg, D., Entry, J., Lentz, R., Orts, W., 2007. Polyacrylamide in agriculture and environmental land management. Advances in Agronomy 92, 75–162.

Sperling, L., 2006. Introduction to Physical Polymer Science, fourth ed. John Wiley & Sons, Inc., Hoboken, NJ.

Stumm, W., Morgan, J., 1996. Aquatic Chemistry: Chemical Equilibria and Rates in Natural Waters, third ed. John Wiley & Sons, Inc., New York, NY.

Sylvia, D., Fuhrmann, J., Hartel, P., Zuberer, D., 2003. Principles and Applications of Soil Microbiology, second ed. Pearson Education Inc., NJ, USA.

Wu, X., Hunkeler, D., Hamielec, A., Pelton, R., Woods, D., 1991. Molecular weight characterization of poly(acrylamide-co-sodium acrylate). I. Viscometry. Journal of Applied Polymer Science 42, 2081–2093.

Zahid, W., Ganczarczyk, J., 1990. Suspended solids in biological filter effluents. Water Research 24, 215–220.